

An experimental, theoretical and kinetic-modeling study of hydrogen sulfide pyrolysis and oxidation

Alessandro Stagni^{*1}, Suphaporn Arunthanayothin^{*2}, Luna Pratali Maffei¹, Olivier Herbinet²,
Frédérique Battin-Leclerc², Tiziano Faravelli¹

¹*Department of Chemistry, Materials, and Chemical Engineering "G. Natta", Politecnico di Milano, Milano 20133, Italy*

²*Laboratoire Réactions et Génie des Procédés, CNRS-Université de Lorraine, 1 rue Grandville, 54000 Nancy, France*

Supplementary Material

Table of contents

1.	Wide-range mechanism validation	4
1.1	Ignition delay times in shock tubes	4
1.1.1	Mathieu et al. [1]	4
1.1.2	Mathieu et al. [2]	5
1.2	Laminar Flame Speed	6
1.3	Flow reactor studies	8
1.3.1	Zhou et al. [11]	8
1.3.2	Song et al. [12]	9
1.3.3	Colom-Díaz et al. [13]	10
1.4	Jet-stirred reactor studies	11
1.4.1	Colom-Díaz et al. [14]	11
2.	Picture of the yellow solid collected when cleaning FR1	13
3.	Supplementary Figures	14
3.1	Repeated JSR oxidation data	14
3.2	Comparison of FR1 and JSR oxidation data	15
4.	Recipe for coating	16
5.	References	17

1. Wide-range mechanism validation

The generality feature of the developed mechanism was later verified against the available literature data in the remaining cases. Hereafter, the capabilities of the model are assessed considering the prediction of ignition delay times in a shock tube and laminar flame speeds, both at atmospheric pressure.

1.1 Ignition delay times in shock tubes

1.1.1 Mathieu et al. [1]

To the authors' knowledge, the only experimental data related to ignition delay times of $\text{H}_2\text{S}/\text{O}_2$ were obtained by Mathieu et al. [1], and were evaluated in an Argon environment (98% vol/vol) at near-atmospheric pressures (0.95 – 1.19 atm) and high temperatures ($1445 \text{ K} \leq T \leq 2210 \text{ K}$), for lean-to-rich equivalence ratios ($0.5 \leq \Phi \leq 1.5$). Results are shown in Figure S1 for the 3 available datasets. The agreement with the experimental data is again reasonably good in lean conditions, while larger deviations observed in richer conditions, especially at lower temperatures (up to ~50% overprediction).

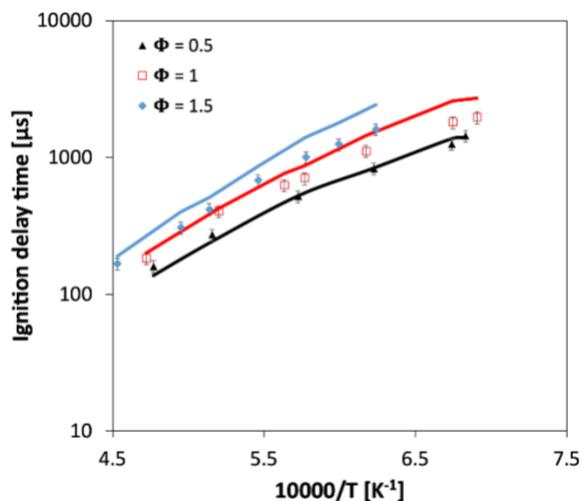


Figure S1. Ignition delay times of $\text{H}_2\text{S}/\text{O}_2$ mixtures in an Argon environment (98% v/v), at near-atmospheric pressures. Experimental [1] and modeling results.

Sensitivity analysis to the H atom, considered as representative of the ignition process, was carried out at comparable temperatures for the different equivalence ratios in order to understand the governing steps, using a common H₂S conversion (1%) as reference. Figure S16 shows the results for each of the initial compositions. In qualitative terms, no significant differences can be identified by varying the equivalence ratio. As also found at lower temperatures in the JSR (Figure S11) and in the two FRs (Figure S14), the ignition process is again governed by the H-abstraction via O₂ (R6b), which activates the radical pool. A key role is also played by the reactions consuming the products of R6b (SH and HO₂), respectively R5 and R11b, ultimately providing, either directly (R5) or indirectly (R11b), H radicals from SH and activating the branching process. In these conditions, the temperatures at stake are also high enough to allow the fuel thermal decomposition (R₁) at a significant rate, such that it appears among the drivers of ignition.

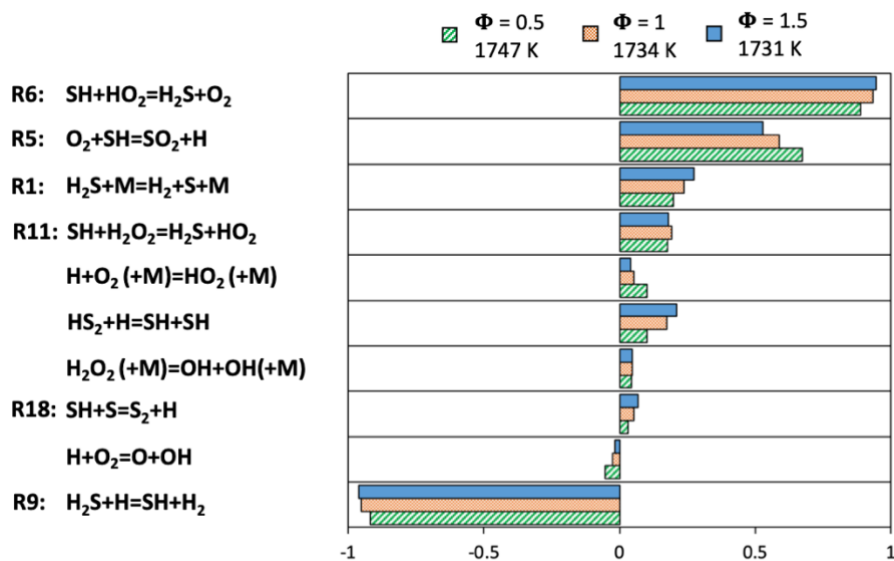


Figure S2. Sensitivity coefficients to H mass fraction, in correspondence of 1% H₂S conversion.

1.1.2 Mathieu et al. [2]

Mathieu et al. [2] measured the effect of the H₂S addition on the ignition delay times of H₂/O₂ mixtures, measured in a shock tube. Different concentrations of H₂S were employed (100, 400, and 1600 ppm) at 3

different pressure levels (1.6, 13, 33 atm) and a wide range of temperature ($1045\text{ K} \leq T \leq 1860\text{ K}$). Modeling results are compared with experiments in Figure S3.

Predictions can be considered as very satisfactory in the whole range of temperatures, pressures and compositions (i.e. amount of added H_2S).

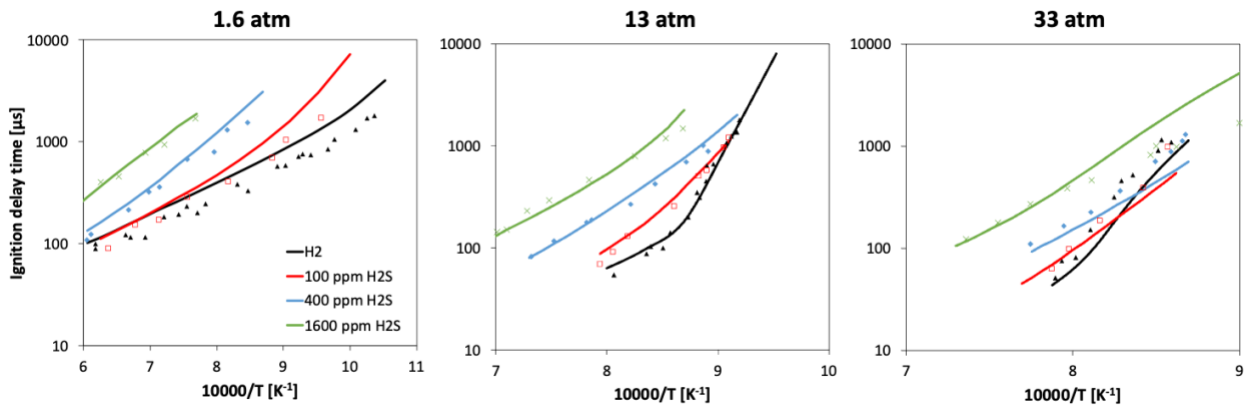


Figure S3. Ignition delay times of 1% H_2 /1% O_2 diluted in Ar, doped with different amounts of H_2S . Experimental [2] and modeling results.

1.2 Laminar Flame Speed

The practical difficulties and safety concerns in managing H_2S already mentioned in the Introduction have strongly limited the execution of experiments involving the measurement of the flame propagation features of such fuel. As a result, to the authors' knowledge no recent experimental campaigns have been performed to evaluate the laminar flame speed of pure H_2S . The only available studies in this regard are either particularly old [3–6] or involve binary mixtures of H_2S with conventional hydrocarbons [3,7]. Nevertheless, for the sake of completeness of the kinetic analysis carried out in this work, the modelling predictions obtained by considering pure H_2S /air mixtures at ambient temperatures and pressure are here compared to the experimental data. In the results shown in Figure S4, the datasets exhibit a significant scattering throughout the whole range of equivalence ratios. In general, the modelling predictions

overestimate the experimental measurements, except in lean conditions when the measurements of Chamberlin and Clarke [4] are considered.

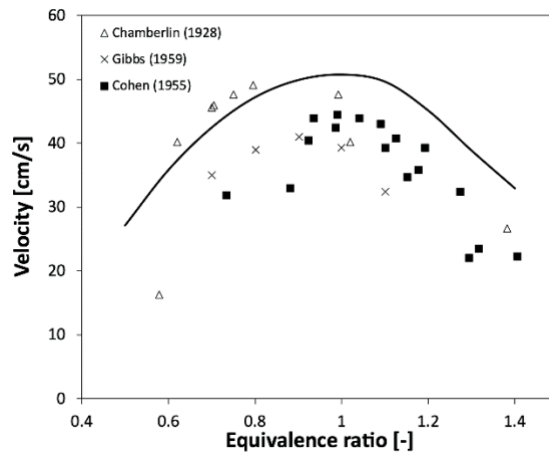


Figure S4. Laminar flame speed of H_2S /air mixtures at atmospheric pressure. $T_{in} = 298$ K. Experimental [4–6] and modeling results.

Beyond the quantitative predictions of the kinetic model, the importance of such evaluation is related to the insight provided by the sensitivity analysis to the laminar flame speed for the different equivalence ratios. Figure S5 highlights the main pathways controlling flame propagation. Unlike in the previous cases, and coherently with what occurs for conventional hydrocarbons [8], the flame velocity is governed by the chemistry of the smallest molecules. In this case, the oxidation of S and SO to SO and SO₂ (via R16 and R17), respectively, acts as the main enhancer of flame propagation, since it provides O radicals to the flame front, and thus causes the radical branching. On the other hand, the termination reactions involving SO and SO₂ with H, O and OH (R22–24) slow down the flame propagation, as well as R1, rather acting as a recombination in correspondence of the flame front.

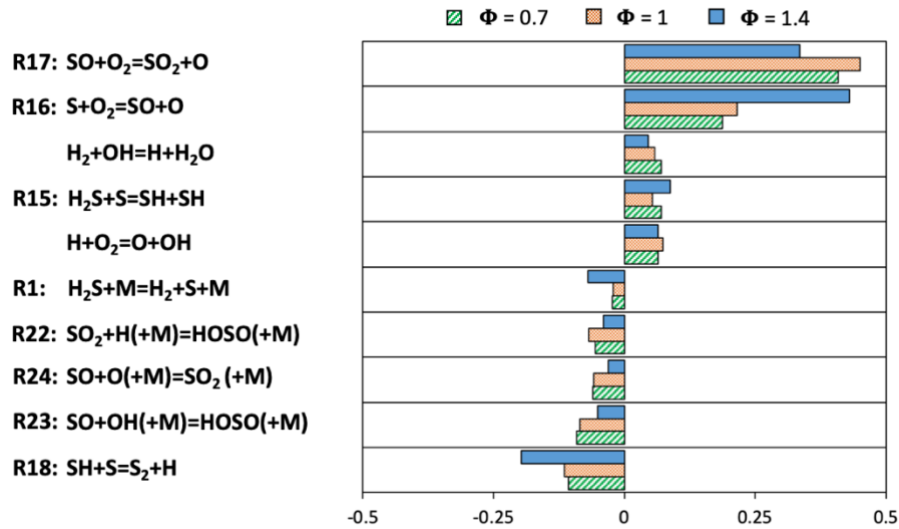


Figure S5. Sensitivity coefficients to the laminar flame speed at $T_{in} = 298 \text{ K}$ and $P = 1 \text{ atm}$ for different Φ .

It can be concluded that the flame propagation features of H_2S is the aspect needing a deeper investigation from both experimental and theoretical sides for such fuel: the availability of up-to-date measurements, with a smaller (and well-defined) uncertainty would provide a useful guide to the kinetic modeling part. At the same time, further theoretical analysis of the oxidation reactions involving S radicals (R16-17) is also desirable. For R16, the calculated rates in the available literature [9,10] are in significant disagreement between each other, while for R17 no theoretical evaluation has been performed so far, to the authors' knowledge.

1.3 Flow reactor studies

1.3.1 Zhou et al. [11]

Zhou et al. [11] carried out flow-reactor experiments of H_2S oxidation in an isothermal flow reactor at $P = 1.05 \text{ bar}$, ($950 \text{ K} \leq T \leq 1150 \text{ K}$), with variable amounts of both H_2S and O_2 (always under fuel-lean conditions). They performed an earlier reactor coating with B_2O_3 , in order to suppress surface effects. Nitrogen was used as balance gas. Modeling predictions are shown in Figure S6 for three different compositions entering the reactor.

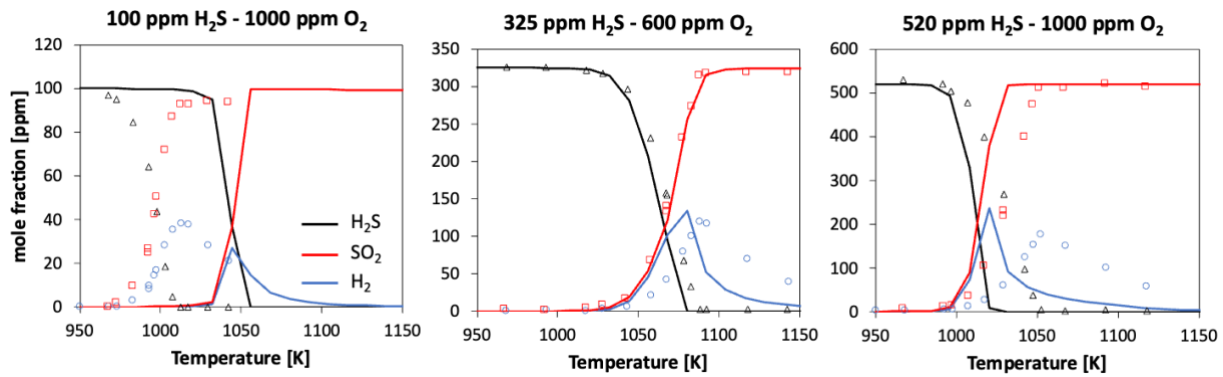


Figure S6. H_2S , SO_2 and H_2 mole fraction profiles at the flow reactor exit, as measured by Zhou et al. [11] at $P = 1.05$ bar. $\tau = 0.2$ s. Balance gas is N_2 . Experimental vs modeling results.

Overall, a reasonable agreement can be observed, although larger overpredictions in the reactivity onset are present with 100 ppm H_2S , in very lean conditions. It is worth highlighting that the predictions by Zhou et al. [11] with their own mechanism (dashed lines in Fig. 3 of [11]) exhibits comparable deviations, too.

1.3.2 Song et al. [12]

Song et al. [12] performed high-pressure oxidation experiments of H_2S/O_2 in an un-coated flow reactor, using a nitrogen environment. They considered 2 pressure levels (30 bar and 100 bar, respectively), a low-temperature range ($450\text{ K} \leq T \leq 900\text{ K}$) and lean ($\Phi = 0.88$) to ultra-lean ($\Phi = 0.028$) conditions. Results and the related modeling predictions are reported in Figure S7.

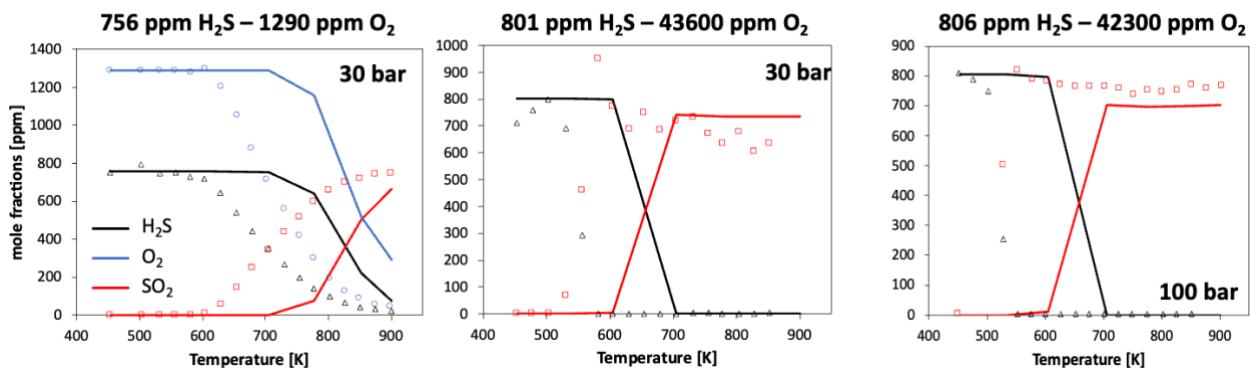


Figure S7. H_2S , O_2 and SO_2 mole fraction profiles at the exit of a flow reactor, as measured by Song et al. [12] at $P = 30$ bar and 100 bar, respectively. Experimental vs modeling results. $\tau = 3520/T[K]$ (left/center) and $\tau = 11700/T[K]$, respectively.

In all of the three cases, overpredictions in the reactivity onset by ~ 100 K can be observed. However, the lack of coating might play a role in the actual conversion rates, as observed by both the work in the present paper and the previous one by Zhou et al. [11] when comparing conversions with and without boric oxide coatings.

1.3.3 Colom-Díaz et al. [13]

Colom-Díaz et al. [13] performed experiments in an un-coated at atmospheric pressure, in very-lean to rich conditions ($0.32 \leq \lambda \leq 19.46$) and $600 \text{ K} \leq T \leq 1400 \text{ K}$. Nitrogen was used as balance gas. Results and modeling predictions are reported in Figure S8.

Overpredictions of the reactivity onset are also observed when modeling such dataset and indicate that the lack of coating might be determining in the conversion rates in this case too.

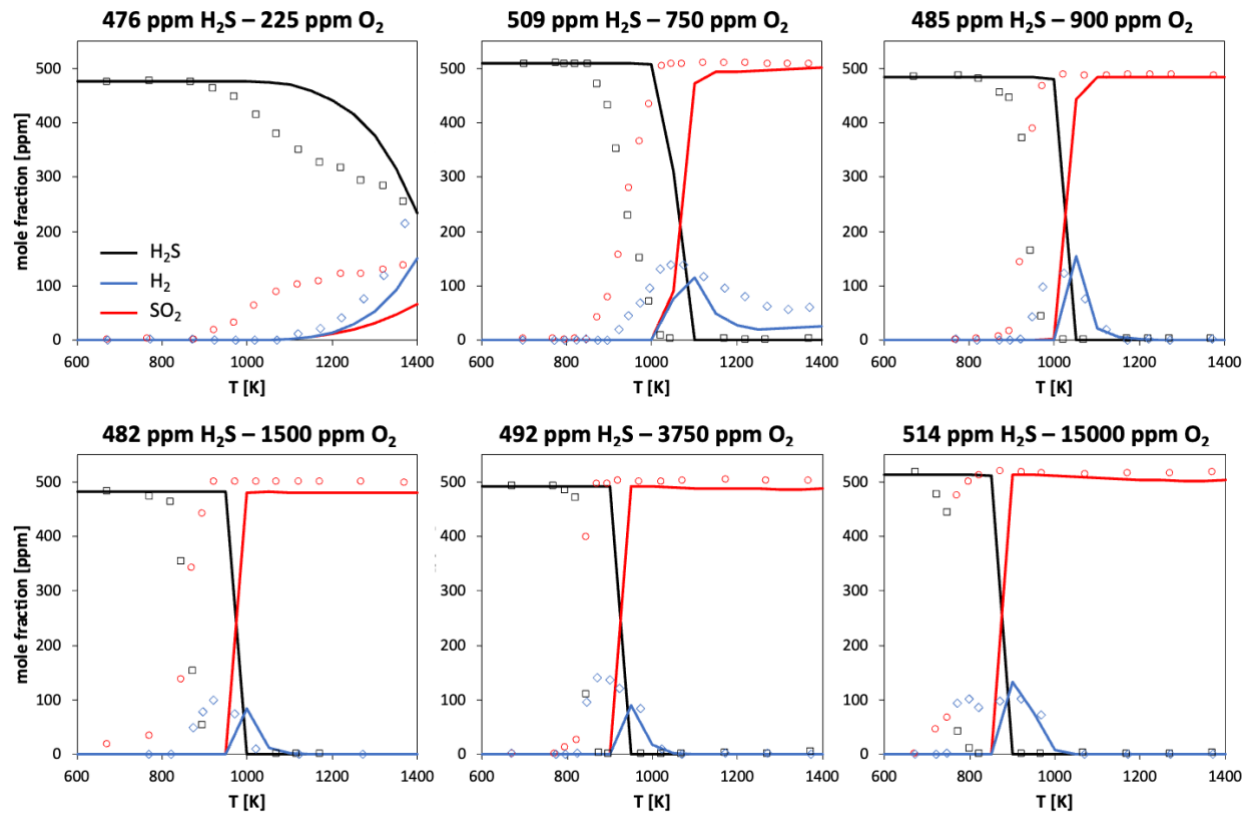


Figure S8. H_2S , H_2 and SO_2 mole fraction profiles at the exit of a flow reactor, as measured by Colom-Díaz et al. [13]. Experiments vs kinetic modeling results.

1.4 Jet-stirred reactor studies

1.4.1 Colom-Díaz et al. [14]

Colom-Díaz et al. [14] studied H_2S oxidation in an un-coated Jet-Stirred Reactor, at atmospheric pressure and in stoichiometric-to-rich conditions ($1 \leq \lambda \leq 5$) and $600 \text{ K} \leq T \leq 1100 \text{ K}$, using nitrogen as balance gas. Residence time was fixed to $\tau = 1 \text{ s}$. Results and modeling predictions are reported in Figure S9. Differently from all the previous cases, the reactivity onset is well predicted by the kinetic model, however a significantly steeper conversion rate (comparable to that observed in the JSR analyzed in this work described in the main paper) can be seen at all the three air/fuel ratios (λ) investigated.

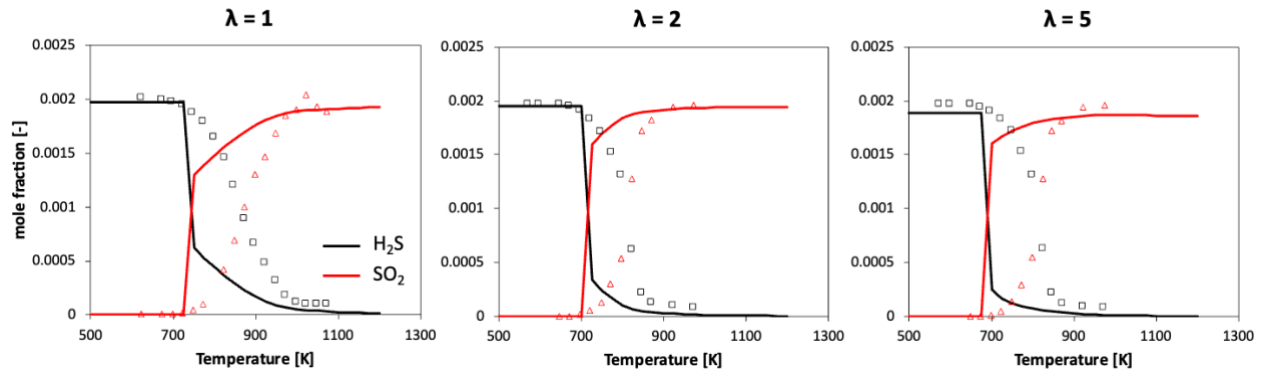


Figure S9. H_2S and SO_2 mole fractions at the exit of a Jet-Stirred Reactor, as measured by Colom-Díaz et al. [14], at atmospheric pressure at three air/fuel ratios. $\tau = 1$ s. Experiments vs modeling results.

2. Picture of the yellow solid collected when cleaning FR1

Figure S10 displays a picture of the yellow solid collected when cleaning the flow reactor FR1 after the study of the pyrolysis and oxidation of H_2S . Yellow crystalline solid is characteristic of elemental sulfur and sulfur allotropes.



Figure S10. Yellow solid collected after the cleaning of FR1.

3. Supplementary Figures

3.1 Repeated JSR oxidation data

JSR oxidation data ($P = 800$ Torr, $\tau = 2$ s, $x_{fuel}^{in} = 800$ ppm, $\Phi = 0.50$) have been repeated twice to check the consistency of experimental data. The tube used for these experiments is a coated alumina tube. The comparison of both sets of experimental data shows a very good agreement.

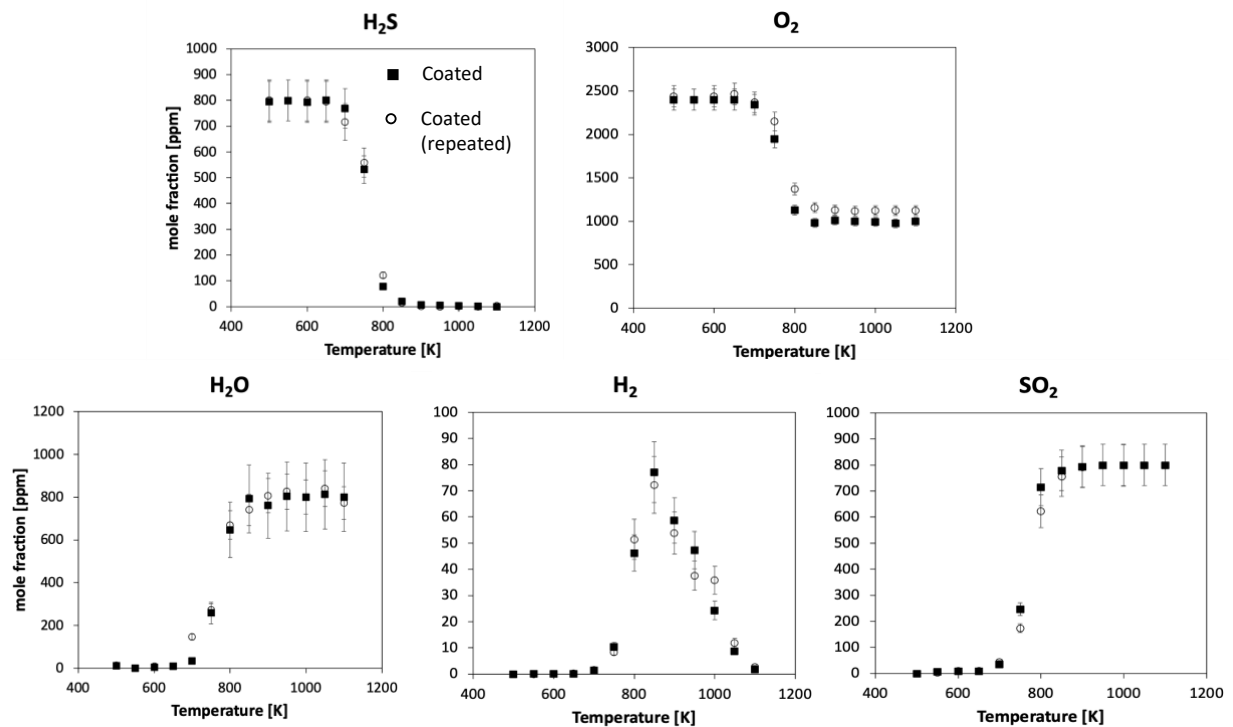


Figure S11. JSR oxidation data ($P = 800$ Torr, $\tau = 2$ s, $x_{fuel}^{in} = 800$ ppm, $\Phi = 0.50$) in a coated reactor. Comparison of two sets of experiments performed in order to check the repeatability.

3.2 Comparison of FR1 and JSR oxidation data

Oxidation data obtained under similar conditions with the JSR and FR1 ($P = 800$ Torr, $\tau = 2$ s in the JSR and ~ 2 s in FR1, $x_{fuel}^{in} = 500$ ppm, $\phi = 0.25$) have been compared. Data are those obtained with coated fused silica reactors. Slight differences are observed (see main text).

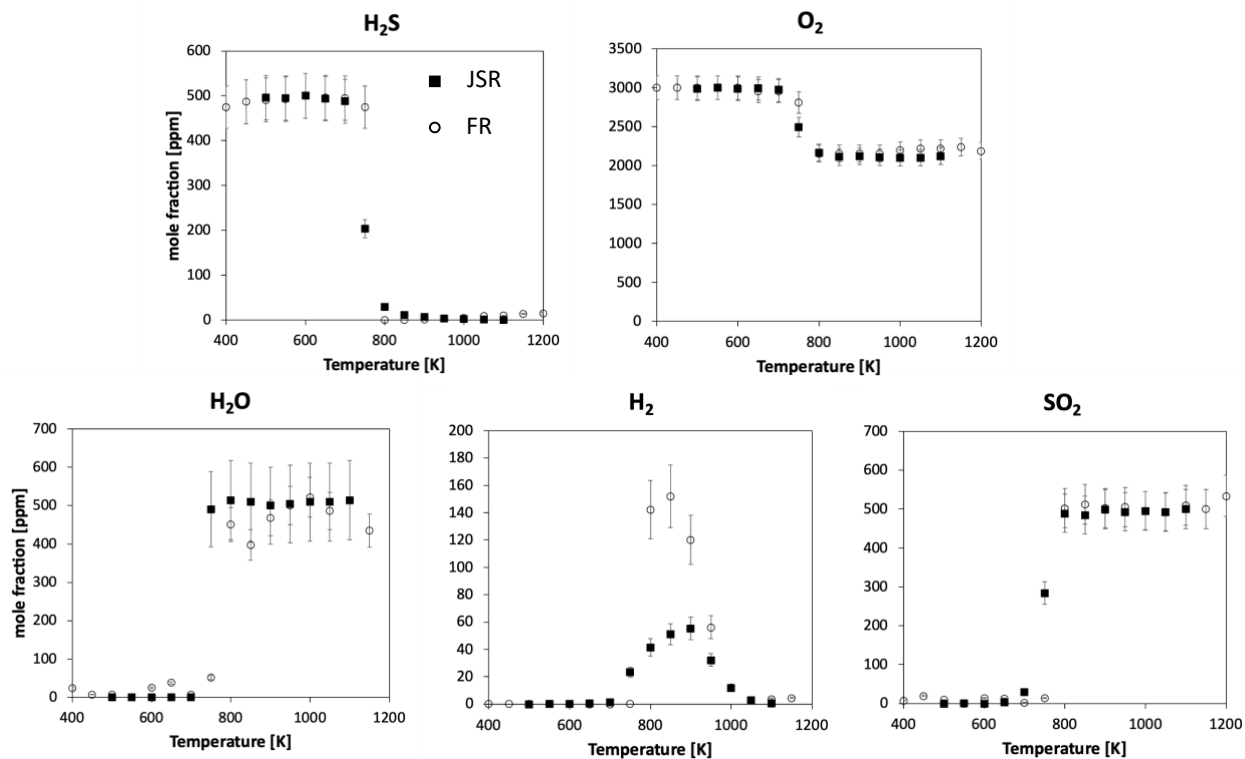


Figure S12. Comparison of JSR and FR1 oxidation data ($P = 800$ Torr, $\tau = 2$ s in the JSR and ~ 2 s in FR1, $x_{fuel}^{in} = 500$ ppm, $\phi = 0.25$) in coated fused silica reactors.

4. Recipe for coating

- 1- A solution of boric acid has been prepared. The solvent is a mixture of acetone and ethanol (50%-50% on a volume base). The solution must be saturated.
- 2- The tube is then filled with the saturated solution. The tube is let with the solution overnight. The tube is drained and dried with helium flowing through. The tube is heated to $\sim 100^{\circ}\text{C}$ to eliminate the remaining solvent molecules. The tube is heated to 500°C to obtain the impervious layer.
- 3- As in the literature, the layer is white and translucent before the heating, invisible after the heating (when silica was used). See for example: A. Egerton, D.R. Warren, Proc. R. Soc. London. Ser. A 204 (1951) 465–476.

5. References

- [1] Mathieu O, Mulvihill C, Petersen EL. Shock-tube water time-histories and ignition delay time measurements for H₂S near atmospheric pressure. *Proc Combust Inst* 2017;36:4019–27.
- [2] Mathieu O, Deguillaume F, Petersen EL. Effects of H₂S addition on hydrogen ignition behind reflected shock waves: Experiments and modeling. *Combust Flame* 2014;161:23–36.
- [3] Kurz PF. Influence of hydrogen sulfide on flame speed of propane-air mixtures. *Ind & Eng Chem* 1953;45:2361–6.
- [4] Chamberlin DS, Clarke DR. Flame Speed of Hydrogen Sulfide. *Ind Eng Chem* 1928;20:1016–8.
- [5] Gibbs GJ, Calcote HF. Effect of Molecular Structure on Burning Velocity. *J Chem Eng Data* 1959;4:226–37.
- [6] Cohen L. Burning velocities of hydrogen sulphide in air and oxygen. *Fuel* 1955;34:S119--S122.
- [7] Mulvihill CR, Keese CL, Sikes T, Teixeira RS, Mathieu O, Petersen EL. Ignition delay times, laminar flame speeds, and species time-histories in the H₂S/CH₄ system at atmospheric pressure. *Proc Combust Inst* 2019;37:735–42.
- [8] Ranzi E, Frassoldati A, Grana R, Cuoci A, Faravelli T, Kelley AP, et al. Hierarchical and comparative kinetic modeling of laminar flame speeds of hydrocarbon and oxygenated fuels. *Prog Energy Combust Sci* 2012;38:468–501.
- [9] Lu C-W, Wu Y-J, Lee Y-P, Zhu RS, Lin M-C. Experiments and calculations on rate coefficients for pyrolysis of SO₂ and the reaction O+ SO at high temperatures. *J Phys Chem A* 2003;107:11020–9.
- [10] Sebbar N, Zirwes T, Habisreuther P, Bozzelli JW, Bockhorn H, Trimis D. S₂+ air combustion: reaction

kinetics, flame structure, and laminar flame behavior. *Energy & Fuels* 2018;32:10184–93.

- [11] Zhou C, Sendt K, Haynes BS. Experimental and kinetic modelling study of H₂S oxidation. *Proc Combust Inst* 2013;34:625–32.
- [12] Song Y, Hashemi H, Christensen JM, Zou C, Haynes BS, Marshall P, et al. An Exploratory Flow Reactor Study of H₂S Oxidation at 30–100 Bar. *Int J Chem Kinet* 2017;49:37–52.
- [13] Colom-Díaz JM, Abián M, Ballester MY, Millera A, Bilbao R, Alzueta MU. H₂S conversion in a tubular flow reactor: Experiments and kinetic modeling. *Proc Combust Inst* 2019;37:727–34.
- [14] Colom-Díaz JM, Alzueta MU, Zeng Z, Altarawneh M, Dlugogorski BZ. Oxidation of H₂S and CH₃SH in a jet-stirred reactor: Experiments and kinetic modeling. *Fuel* 2021;283:119258.